<Advanced Research Center for Beam Science>Electron Microscopy and Crystal Chemistry

Advanced Research Center for Beam Science – Electron Microscopy and Crystal Chemistry –

http://eels.kuicr.kyoto-u.ac.jp:8080/Root/English

Prof
KURATA, Hiroki
(D Sc)

Assist Prof
NEMOTO, Takashi
(D Sc)

Assist Prof
HARUTA, Mitsutaka
(D Sc)

Program-specific Res*
OGAWA, Tetsuya
(D Sc)

Program-specific Res*
KIYOMURA, Tsutomu

*Nanotechnology Platform

Assist Techn Staff

HIRAIZUMI, Yuri

Students

FUJIYOSHI, Yoshifumi (D3)
YAMAGUCHI, Atsushi (D2)
LAI, Ming Wei (D1)
TOMISAKI, Yuriko (M2)
INOUE, Shota (M1)

Scope of Research

We study crystallographic and electronic structures of materials and their transformations through direct imaging of atoms or molecules by high-resolution electron spectromicroscopy, which realizes energy-filtered imaging and electron energy-loss spectroscopy as well as high-resolution imaging. By combining this with scanning probe microscopy, we cover the following subjects: 1) direct structure analysis, electron crystallographic analysis, 2) epitaxial growth of molecules, 3) structure formation in solutions, and 4) fabrication of low-dimensional functional assemblies.

KEYWORDS
AREELS
Surface Plasmon
Dispersion Relation
Waveguide
Transverse Magnetic Mode

Selected Publications

Minari, T.; Nemoto, T.; Isoda, S., Temperature and Electric-field Dependence of the Mobility of a Single-grain Pentacene Field-effect Transistor, *J. Appl. Phys.*, **99,** [034506-1]-[034506-5] (2006).

Haruta, M.; Kurata, H.; Komatsu, H.; Shimakawa, Y.; Isoda, S., Site-resolved Oxygen K-edge ELNES of Layered Double Perovskite La_2CuSnO_6: *Physical Review B*, **80,** [165123-1]-[165123-6] (2009).

Haruta, M.; Kurata, H., Direct Observation of Crystal Defects in an Organic Molecular Crystals of Copper Hexachlorophthalocyanine by STEM-EELS, *Sci. Rep.*, **2,** [252-1]-[252-4] (2012).

Aso, R.; Kan, D.; Shimakawa, Y.; Kurata, H., Atomic Level Observation of Octahedral Distortions at the Perovskite Oxide Heterointerface, *Sci. Rep.*, **3,** [2214-1]-[2214-6] (2013)

Saito, H.; Namura, K.; Suzuki, M.; Kurata, H., Dispersion Relations for Coupled Surface Plasmon-polariton Modes Excited in Multilayer Structures, *Microscopy*, **63,** 85-93 (2014)

Formation of a Hybrid Plasmonic Waveguide Mode Probed by Dispersion Measurement

Guiding light with subwavelength confinement is a critical challenge for nanoscale optical applications. Hybrid waveguides, i.e., dielectric waveguides combined with plasmonic waveguides, have great potential for concomitantly exhibiting subwavelength confinement and long range propagation, enabling a highly integrated photonic circuit. This waveguide mode has been regarded as a coupling of the dielectric waveguide and the surface plasmon-polaritons (SPPs). We report the characterization of hybrid waveguide modes excited in $Si/SiO_2/Al$ films by dispersion measurement using angle-resolved electron energy-loss spectroscopy (AREELS).

Figure 1(a) shows a schematic diagram of AREELS. A narrow slit is placed to be perpendicular to the direction of energy dispersion for the spectrometer at the entrance plane where the angular dispersive (electron diffraction) pattern is formed. The observed two-dimensional AREELS pattern allows us to directly visualize the energy-loss probability as a function of the energy loss E and the component of the scattering vector perpendicular to the direction of incident electrons $q_\perp$ (E–q map). When the incident electrons are normal to the multilayered films, $q_\perp$ can be assumed to be the wave vector k (propagation constant) of the propagating waves in waveguide structures. Therefore, the E–q map directly yields the dispersion relations of the waveguide modes.

The waveguide structures consisting of the multilayered semiconductor–insulator (SI) and semiconductor–insulator–metal (SIM) films were prepared as shown in Figure 1(b). Silicon (Si), silicon dioxide (SiO_2), and aluminum (Al) were chosen as the semiconductor layer, the insulator gap, and the metal layer, respectively. Since the SPP mode supported by the plane surface is the transverse magnetic (TM) mode, we consider the dispersion relations for TM modes only in the present study.

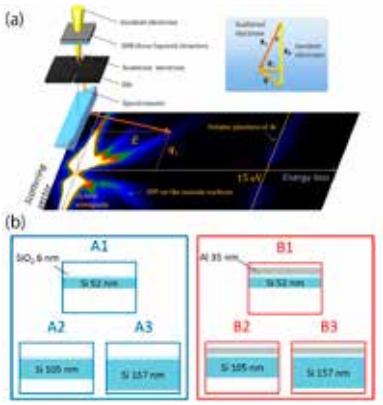

Figure 1. (a) Schematic diagram of AREELS method. k_0 and k_1 represent the wave vectors of incident and scattered electrons, respectively. An angular selection slit is placed at the entrance plane of the spectrometer to limit electron collection to those scattered perpendicular to the direction of energy dispersion. The gap in the center of the slit is closed to prevent the intense direct beam from saturating the CCD detector. The inserted E–q map is taken from B2. (b) Schematics of the specimens.

Figure 2 shows the E–q maps of the SI films (A1, A2, and A3) and SIM films (B1, B2, and B3), in which they are compared with the calculated dispersion relations of light in vacuum, bulk amorphous SiO_2, and Si crystal (white solid lines and curves). On the E–q map in Figure 2(b), the dispersion curve of the lowest TM mode (TM_0) appears in the region between the light lines in vacuum and Si bulk. This is a feature of Si waveguide modes. When the thickness of the Si film is increased, dispersion curves of two TM modes are observed, as shown in Figure 2(c). The dispersion curve of the TM_0 mode shifts to the lower energies with increasing Si thickness. This behavior is characteristic of dielectric waveguide modes. Figures 2(d)–2(f) show the E–q maps measured from SIM films (B1, B2, and B3). A new dispersion curve clearly appears in the E–q map of Figure 2(d), whereas no dispersion curve was detected for the corresponding SI film (A1), as seen in Figure 2(a). This dispersion curve might be related to the SPP excited on the Al/SiO_2 interface. Moreover, when the thickness of the Si film in SIM structures is increased, the dispersion curves shift to lower energies (see Figure 2(e) and 2(f)), similar to SI films. The new peaks observed in the SIM film (B2) are lower than those of the Si waveguide (TM_0) mode in the SI film (A2), which suggests that the new excitation mode arises from the coupling between the SPPs on the Al/SiO_2 interface and the TM_0 modes in the Si film, representing a hybrid waveguide mode.

A hybrid mode can be characterized in terms of the effective index, defined as the propagation constant of waveguide mode divided by the wave vector in vacuum. With increasing Si waveguide layer thickness, the critical energy, where effective indexes of the TM_0 and SPP modes intersect, giving maximum coupling seems to decrease, which suggests that the energy of effective hybrid coupling can be controlled by adjusting the thickness of the dielectric waveguide layer.

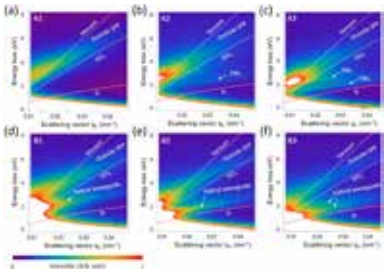

Figure 2. E–q maps of (a) A1, (b) A2, (c) A3, (d) B1, (e) B2, and (f) B3. White solid curves and lines are calculated dispersion relations of light in bulk Si, bulk SiO_2, and vacuum. The red curve represents the relationship between the energy and $q_\perp$ of Čerenkov radiation excited by 200 keV electrons in bulk Si.